Planta (2007) 226:1067–1073
DOI 10.1007/s00425-007-0564-5

RAPID COMMUNICATION

The *pds2* mutation is a lesion in the *Arabidopsis* homogentisate solanesyltransferase gene involved in plastoquinone biosynthesis

Li Tian · Dean DellaPenna · Richard A. Dixon

Received: 19 April 2007 / Accepted: 24 May 2007 / Published online: 14 June 2007

Abstract Plastoquinone plays critical roles in photosynthesis, chlororespiration and carotenoid biosynthesis. The previously isolated *pds2* mutant from *Arabidopsis* was deficient in tocopherol and plastoquinone accumulation, and the biochemical phenotype of this mutant could not be reversed by externally applied homogentisate, suggesting a later step in tocopherol and/or plastoquinone biosynthesis had been disrupted. Recently, the protein encoded by At3g11950 (*AtHST*) was shown to condense homogentisate with solanesyl diphosphate (SDP), the substrate for plastoquinone synthesis, but not phytyl diphosphate (PDP), the substrate for tocopherol biosynthesis. We have sequenced the *AtHST* allele in the *pds2* mutant background and identified an in-frame 6 bp (2 aa) deletion in the gene. The *pds2* mutation could be functionally complemented by constitutive expression of *AtHST*, demonstrating that the molecular basis for the *pds2* mutation is this 6 bp-lesion in the *AtHST* gene. Confocal microscopy of EGFP tagged AtHST suggested that AtHST is localized to the chloroplast envelope, supporting the hypothesis that plastoquinone synthesis occurs in the plastid.

Keywords Homogentisate · *pds2* · Plastoquinone · Prenyltransferase · Solanesyl diphosphate

L. Tian · R. A. Dixon (✉)
Plant Biology Division, The Samuel Roberts Noble Foundation, 2510 Sam Noble Parkway, Ardmore, OK 73401, USA
e-mail: radixon@noble.org

D. DellaPenna
Department of Biochemistry and Molecular Biology, Michigan State University, East Lansing, MI 48824, USA

Abbreviations

EGFP	Enhanced green fluorescence protein
HGA	Homogentisate
HGGT	Homogentisate geranylgeranyltransferase
HPP	Hydroxyphenylpyruvate
HPPDase	Hydroxyphenylpyruvate dioxygenase
HPT	Homogentisate phytyltransferase
HST	Homogentisate solanesyltransferase
PDP	Phytyl diphosphate
PQ-9	Plastoquinone-9
SDP	Solanesyl diphosphate
SPS	Solanesyl diphosphate synthase

Introduction

Plastoquinone is located in the thylakoid and envelope membranes of the chloroplast and acts as an electron carrier in the light-dependent reactions of photosynthesis (Soll et al. 1980). Plastoquinone is also involved in the chlororespiratory pathway catalyzed by plastoquinone oxidoreductase, and as an electron carrier in carotenoid biosynthesis (Norris et al. 1995; Nievelstein et al. 1995). Plastoquinone consists of an aromatic head group derived from homogentisate (HGA), and an isoprenoid side chain derived from solanesyl diphosphate (SDP). HGA is produced from hydroxyphenylpyruvate (HPP) by the action of hydroxyphenylpyruvate dioxygenase (HPPDase) (Garcia et al. 1997). SDP is synthesized from condensation of nine isoprene units, catalyzed by solanesyl diphosphate synthase (SPS) (Hirooka et al. 2003). HGA and SDP are condensed by homogentisate solanesyltransferase (HST) to form 2-demethylplastoquinol-9, which is then methylated and oxidized to form plastoquinone-9 (PQ-9) (Fig. 1).

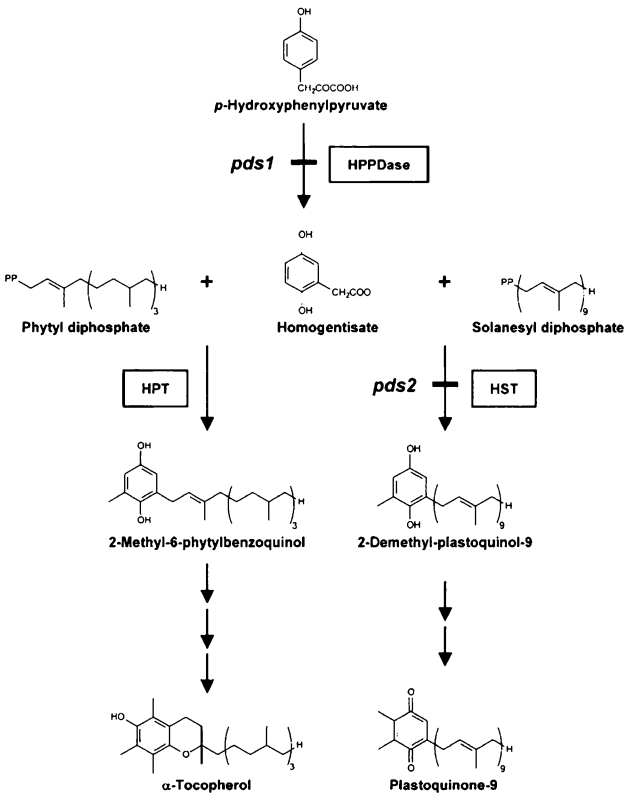

Fig. 1 Biosynthesis of plastoquinone-9 and α-tocopherol in higher plants. The steps blocked by the *pds1* and *pds2* mutations in *Arabidopsis* are indicated. *HPPDase* hydroxyphenylpyruvate dioxygenase; *HPT* homogentisate phytyltransferase; *HST* homogentisate solanesyltransferase

In an earlier forward genetics screening for *Arabidopsis* mutants that were disrupted in carotenoid biosynthesis, two non-allelic albino mutants, *pds1* and *pds2*, were identified, both of which accumulated phytoene and were deficient in plastoquinone and tocopherol (Norris et al. 1995). The fact that neither mutation mapped to the *Arabidopsis* phytoene desaturase locus suggested that PDS1 and PDS2 were required for electron transport associated with phytoene desaturation. The albino phenotype of the *pds1* mutant plants could be rescued by growth on HGA, and the *PDS1* gene was cloned from *Arabidopsis* and shown to encode HPPDase (Norris et al. 1995, 1998).

Homogentisate is the common substrate for the prenylation steps of tocopherol and plastoquinone biosyntheses in the chloroplasts of higher plants (Fig. 1). Because both tocopherol and plastoquinone levels were below detection in the *pds2* mutant, it was proposed that *pds2* might be a lesion in a prenyltransferase gene required for the biosyntheses of both tocopherols and plastoquinone. In an attempt to clone the *Arabidopsis PDS2* locus (mapped to chromosome 3) by a genomics approach, the gene encoding homogentisate phytyltransferase (AtHPT) was identified from *Arabidopsis* and Synechocystis (Collakova and DellaPenna 2001; Savidge et al. 2002). AtHPT belongs to the UbiA aromatic prenyltransferase family, contains a conserved prenyl diphosphate binding motif and specifically catalyzes the condensation of HGA and phytyl diphosphate (PDP), forming the first committed intermediate in tocopherol synthesis, 2-methyl-6-phytylbenzoquinol (Siebert et al. 1992; Collakova and DellaPenna 2001; Savidge et al. 2002). Because *AtHPT* is localized on chromosome 2, does not utilize SDP as a substrate and disruption of the gene eliminates tocopherol synthesis without affecting plastoquinone synthesis, it was concluded that *PDS2* was not an AtHPT and that distinct prenyltransferases were required for tocopherol and plastoquinone synthesis (Collakova and DellaPenna 2001; Savidge et al. 2002).

Using a bioinformatics-based approach, a gene encoding HST was identified and characterized from *Arabidopsis* (Sadre et al. 2006; Venkatesh et al. 2006). Like AtHPT, AtHST (At3g11950) also contained conserved motifs that place it in the UbiA family of aromatic prenyltransferases. In vitro enzyme assays with *E. coli* membrane fractions containing recombinant AtHST protein showed that the enzyme specifically condensed SDP and HGA to produce the predicted prenylated PQ-9 biosynthetic intermediate, 2-demethyl plastoquinol-9 (Sadre et al. 2006). Overexpression of *AtHST* in wild type *Arabidopsis* led to a modest increase in PQ-9 levels in the transgenic plants compared to the controls (Sadre et al. 2006). Interestingly, ectopic expression of AtHST in *Arabidopsis* had a pleiotropic effect on tocopherol accumulation, as the level of tocopherols increased in both leaves and seeds of the transgenic plants (Sadre et al. 2006; Venkatesh et al. 2006).

The chromosomal location of AtHST, its specific prenyltransferase activity in plastoquinone synthesis, and the biochemical phenotype of AtHST transgenic plants, suggested that a disruption in the AtHST gene might account for the *pds2* mutant phenotype. We here report the identification of an in-frame 6 bp deletion in *AtHST* in the *pds2* mutant background, functional complementation of *pds2* by overexpressing an *AtHST* cDNA and subcellular localization of the AtHST protein.

Materials and methods

Plant materials

Arabidopsis thaliana (ecotype Columbia) and tobacco (*Nicotiana tobacum* NC Cornell) plants were used in this study. *Arabidopsis* seeds were sewn on soil and stratified at 4°C for 3 days before transfer to a growth chamber (16 h light 22°C/8 h dark 19°C cycle). Tobacco plants used for the transient expression study were grown

under previously described conditions (Tian and Dixon 2006).

Genomic DNA isolation and sequence analysis

All of the PCR reactions for sequencing and subsequent cloning were performed using high fidelity Pfu DNA polymerase (Stratagene, La Jolla, CA, USA) and the correctness of all cloned, amplified products was confirmed by DNA sequencing. Immature albino *pds2* seedlings were germinated on Murashige and Skoog (MS) plus 3% sucrose agar plates (Murashige and Skoog 1962). Genomic DNA from homozygous *pds2* seedlings and corresponding wild type *Arabidopsis* (ecotype Wassilewskija, Ws) was extracted using the Qiagen DNeasy Plant mini kit (Qiagen, Valencia, CA, USA). The primers used for amplification and sequencing of the coding region of *AtHST* (At3g11950) in Ws and *pds2* are listed in Table 1. Three independent sets of PCR reactions were performed for each amplification, the reactions were pooled, gel purified and used as templates for sequencing. DNA sequencing was performed on an ABI 3700 sequence analyzer (Applied Biosystems, Foster City, CA, USA). DNA sequence analysis was done using the Lasergene DNA Star software (Skirball Institute of Biomolecular Medicine, New York City, NY, USA). Multiple sequences were aligned with ClustalX (Thompson et al. 1997; http://www-igbmc.u-strasbg.fr/BioInfo/ClustalX/Top.html) and edited using GeneDoc (Nicholas et al. 1997; http://www.psc.edu/biomed/genedoc).

Complementation of the *Arabidopsis pds2* mutation

All of the restriction enzymes used for digestions were purchased from New England Biolabs (Boston, MA, USA). The open reading frame of AtHST was amplified with 5′-CGGAATTCATGGAGCTCTCGAT-3′ and 5′-GGGGTACCCTAGAGGAAGGGGAATA-3′ primers, digested with *Eco*RI and *Kpn*I, and ligated to *Eco*RI and *Kpn*I digested pRTL2 vector (Restrepo et al. 1990). The pRTL2-AtHST plasmid was digested with *Hind*III, and the *Hind*III fragment containing *AtHST* under the control of a double 35S promoter and a nos terminator was ligated into *Hind*III-digested pCAMBIA3300 vector. pCAMBIA3300-AtHST was transformed into *Agrobacterium* LBA4404 competent cells (Invitrogen, Carlsbad, CA, USA) by electroporation. *Agrobacterium* containing pCAMBIA3300-AtHST was transformed into *Arabidopsis* plants heterozygous for the *pds2* mutation by the floral dip method (Clough and Bent 1998).

Table 1 Sequences of primers used for amplification and sequencing of *AtHST* in the Ws and *pds2* backgrounds

Orientation	Sequence
Forward 1	5′-GGAATCAAGATCTCACCCAAAAA-3′
Forward 2	5′-ATGGAGCTCTCGATCTCACAA-3′
Forward 3	5′-AAACAACATCTTATCTTACT-3′
Forward 4	5′-TTGCCACGGTAAATGCTGTT-3′
Forward 5	5′-GCTTCAGGCTTAATTTTCCAGGTA-3′
Reverse 1	5′-GAGGAAGGGGAATAACAGATA-3′
Reverse 2	5′-GAGCGGAAAGAAAATGGTTATGC-3′
Reverse 3	5′-TAAATAATAATAGTGACCAA-3′

Transformed *Arabidopsis* plants were selected for resistance to Basta (the active ingredient is glufosinate). Genomic DNA from the leaves of Basta-resistant plants was extracted and used as template for PCR reactions to specifically amplify a fragment of AtHST spanning the 6 bp *pds2* deletion (primers 5′-CACTTTCAGGTCTTCTTGCTCT-3′ and 5′-GTGCTGCATACTTGTCG-3′). The Basta-resistant, *pds2* heterozygous T1 plants were identified based on the different amplicon sizes resulting from the 6 bp deletion in the *pds2* allele, and were allowed to self-pollinate. Developing embryos in siliques of mature T1 plants were scored for green to white ratio as previously described (Norris et al. 1995). The T2 seeds were also collected at maturity and plated on MS2 plates (Norris et al. 1995) with glufosinate (at 10 mg/l) to determine Basta resistance.

Transient expression and confocal microscopy

An in-frame fusion of *AtHST* and the *EGFP* gene was generated by two-step PCR as previously described (Tian and Dixon 2006). The open reading frames of *AtHST* and *EGFP* were amplified with 5′-CGGAATTCATGGAGCTCTCGAT-3′ and 5′-GCCCTTGCTCACCAT/GAGGAAGGGGAATAA-3′ primers and 5′-TTATTCCCCTTCCTC/ATGGTGAGCAAGGGC-3′ and 5′-AGTTATCTAGAGTCGCGGCC-3′ primers, respectively. One μl of each of the first step PCR reactions was used as template for the second step amplification with 5′-CGGAATTCATGGAGCTCTCGAT-3′and 5′-AGTTATCTAGAGTCGCGGCC-3′ primers. The second step PCR reaction product was gel-purified, digested with *Eco*RI and *Xba*I, and ligated to *Eco*RI and *Xba*I digested pRTL2 vector.

About 5 μg of pRTL2-AtHST-EGFP DNA was coated with gold particles as previously described (Liu and Dixon 2001). The particle gun (DuPont, Wilmington, DE, USA) was fired at 1100 psi. Epidermal cells of young tobacco plants (*Nicotiana tobacum*, NC Cornell) transfected with the pRTL2-AtHST-EGFP plasmid were examined 18 h after particle bombardment. The fluorescence images were recorded on a Leica TCS SP2 AOBS confocal laser scanning microscope system (Leica, Bannockburn, IL, USA) and saved as TIFF files. The TIFF images were assembled using the Adobe Photoshop software (Adobe Systems, San Jose, CA, USA).

Results and discussion

Through bioinformatics-based motif analysis, At3g11950 was initially identified as a paralog of *VTE2* (*AtHPT*), the prenyltransferase involved in tocopherol synthesis in *Arabidopsis* (Venkatesh et al. 2006). Subsequent biochemical analysis using different prenyl diphosphate substrates showed that At3g11950 encoded AtHST, an enzyme in PQ synthesis that specifically condenses SDP and HGA (Sadre et al. 2006). *AtHST* maps to the same chromosomal region on chromosome 3 as the *Arabidopsis pds2* mutation, which has not yet been characterized.

The *Arabidopsis pds2* mutation is a lesion in the *AtHST* gene

To determine the molecular basis of the *pds2* mutation, genomic sequences of *AtHST* from wild type Ws and the *pds2* mutant were determined by DNA sequencing. Comparison with the wild type *AtHST* sequence revealed an in-frame 6 bp deletion (corresponding to Val148 and Gly149) in the coding region of *AtHST* in *pds2* (Fig. 2). AtHST belongs to the UbiA family of prenyltransferases. No crystal structure of UbiA or other aromatic prenyltransferases has been determined to date, but by using secondary structure predication and homology-based modeling with the photosynthetic reaction center protein of *Rhodopseudomonas virdis* as template, a putative structure was derived for *E. coli* UbiA prenyltransferase (Bräuer et al. 2004). Further refinement of the structure and docking studies with various substrate analogs suggested that it had two predicted active site with putative active site 1, at the N-terminus of the enzyme, proposed to be where the 4-hydroxybenzoate and prenyldiphosphate substrates bind and the prenylation reaction occurs (Bräuer et al. 2004).

Plant aromatic prenyltransferases and bacterial UbiA prenyltransferases share low homology at the amino acid sequence level, with the exception of the conserved catalytic domain (Venkatesh et al. 2006). To determine the location of Val148 and Gly149 in AtHST (deleted in the *pds2* allele) relative to the *E. coli* UbiA prenyltransferase active sites, selected plant aromatic prenyltransferases, all of which use homogentisate as the prenyl acceptor, and bacterial and archaeal UbiA prenyltransferases, which use other aromatic compounds as prenyl acceptors, were aligned using the ClustalX program (Thompson et al. 1997; Fig. 2). The multiple sequence alignment showed that the putative active site 1 in the *E. coli* UbiA prenyltransferase was highly conserved among all the prenyltransferases analyzed (Fig. 2). Val148 and Gly149 are located at the beginning of the conserved putative active site 1 and are conserved in the plant aromatic prenyltransferases, but not in the bacterial and archaeal UbiA enzymes. The conservation and location of Val148 and Gly149 adjacent to the conserved active site of aromatic prenyltransferases may explain the severe impact that deletion of these two amino acids has in the *Arabidopsis pds2* mutant. Because plant aromatic prenyltransferases and bacterial UbiA prenyltransferases share a similar prenylation reaction mechanism but utilize different aromatic and prenyl diphosphate substrates, this suggests that the two amino acids deleted in *pds2* are important for substrate binding, rather than general catalysis.

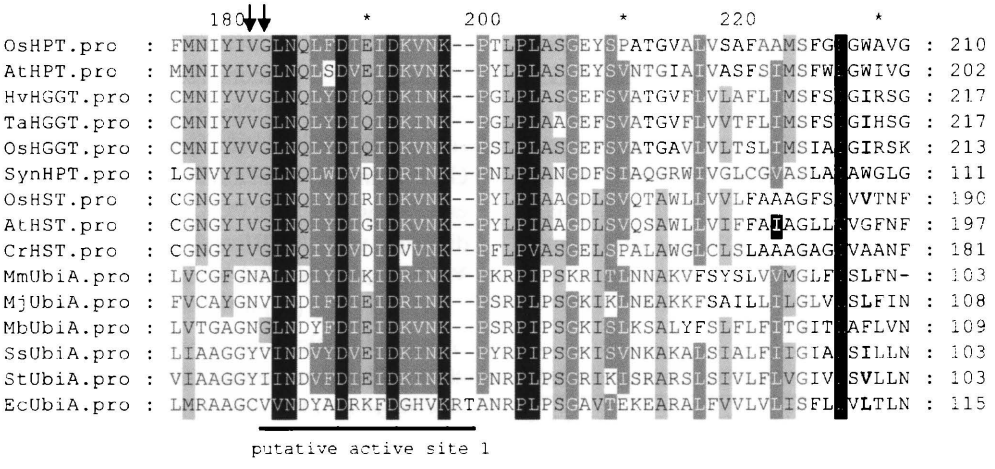

Fig. 2 Multiple sequence alignment of selected aromatic prenyltransferases from plant, bacteria and archaea. Putative active site 1 in the *E. coli* UbiA prenyltransferase predicted by Bräuer et al. (2004) is *underlined*. The conserved amino acids Val and Gly (deleted in the *Arabidopsis pds2* allele) in plant aromatic prenyltransferases are indicated by *arrows*. At, *Arabidopsis thaliana*; Cr, *Chlamydomonas reinhardtii*; Ec, *Escherichia coli*; Hv, *Hordeum vulgare*; Mb, *Methanococcoides burtonii*; Mj, *Methanocaldococcus jannaschii*; Mm, *Methanococcus maripaludis*; Os, *Oryza sativa*; Ss, *Sulfolobus solfataricus*; St, *Sulfolobus tokodaii*; Syn, *Synechocystis sp.* PCC6803; Ta, *Triticum aestivum*. The GenBank accession numbers are: AtHPT, NM_179653; AtHST, NP_187801; CrHST, AM285678; EcUbiA, AP_004541; HvHGGT, AY222860; MbUbiA, ZP_00148041; MjUbiA, NP_247252; MmUbiA, NP_988797; OsHGGT, AY222862; OsHPT, BAD38343; OsHST, XP_478828; SsUbiA, NP_342106; StUbiA, NP_377411; SynHPT, CAC18911; TaHGGT, AY222861

Complementation of the *pds2* mutation with *AtHST*

To determine whether the *pds2* mutation can be functionally complemented by *AtHST*, the open reading frame of *AtHST* was constitutively overexpressed under the double 35S promoter in *Arabidopsis* plants heterozygous for the *pds2* mutation. Thirty Basta resistant T1 transformants were selected and screened for presence of the *pds2* mutation by PCR. The Basta resistant T1 plants that were also heterozygous for *pds2* were allowed to self-pollinate and developing embryos in siliques of the mature T1 plants were scored for their green to white ratio. If the *AtHST* cDNA was able to complement the *pds2* mutation, a 15:1 green to white embryo ratio would be expected in the progeny of the heterozygous transformed plants, whereas if *pds2* was not complemented by the transgene, a 3:1 green to white embryo ratio would be expected. Segregation analysis of three representative lines is shown in Table 2. The green to white embryo ratio was statistically significant for an expected 15:1 ratio, indicating that *AtHST* did complement the *pds2* mutation in vivo and demonstrating that PDS2 is indeed AtHST. The T2 seeds of all three lines segregated for a single transgenic locus as indicated by Basta segregation (Table 2).

Intracellular localization of AtHST

AtHST contains a putative 69 aa chloroplast transit peptide at its N-terminus, as determined by the TargetP program (Nielsen et al. 1997; Emanuelsson et al. 2000), indicating the possible chloroplast localization of the protein. To determine the subcellular localization of AtHST, the open reading frame of *EGFP* was fused in-frame to the C-terminus of *AtHST*, and subcloned in the pRTL2 vector under the control of a double 35S promoter. The pRTL2-*AtHST-EGFP* construct was used for transient expression analysis in tobacco. Young leaves of tobacco plants were transfected with gold particles coated with the pRTL2-*AtHST-EGFP* plasmid DNA. Eighteen hours after biolistic bombardment, the green fluorescence from EGFP and red chlorophyll autofluorescence were monitored by laser scanning confocal microscopy. The emission of green fluorescence was collected at 500–535 nm and the red fluorescence was collected at 555–700 nm. The overlaid image of green fluorescence from EGFP and red autofluorescence from chlorophyll clearly indicated that AtHST was specifically associated with chloroplasts, and there was no direct correlation between green and red fluorescence (Fig. 3c). Notably, the green fluorescence was predominantly localized to the chloroplast envelope as shown in the overlaid image of red and green fluorescence (Fig. 3f).

There have been conflicting reports on the subcellular localization of the plastoquinone biosynthetic enzymes and reactions. Isolated Golgi vesicles from spinach leaves were enriched for HST activity (Swiezewska et al. 1993; Osowska-Rogers et al. 1994; Wanke et al. 2000) and it was proposed that plastoquinone was synthesized in the endoplasmic reticulum/Golgi system and then transferred to its final location in the chloroplast (Swiezewska 2004). In contrast, Soll et al. used isolated enriched inner and outer membrane fractions from spinach chloroplasts to show that the HST catalyzed reaction and final methyltransferase reaction in PQ synthesis were localized to the inner envelope membrane (Soll et al. 1985). Recently, two *Arabidopsis* solanesyl diphosphate synthases were cloned and their subcellular localizations analyzed (Hirooka et al. 2003; Hirooka et al. 2005). The localization of AtSPS1 was inconclusive based on imaging of an AtSPS1-GFP fusion protein, but imaging of the AtSPS2-GFP fusion protein showed that AtSPS2 was targeted to the chloroplast and it was hypothesized to localize in the chloroplastic stroma based on the lack of any transmembrane domain in the protein and the optimal enzyme activity at pH 8.0 (Hirooka et al 2005). Our confocal images of the AtHST-EGFP fusion protein clearly indicate that the AtHST protein is located in the chloroplast, most likely on the envelope membrane (Fig. 3).

Taken together, the map location of *AtHST*, DNA sequence analysis of the *pds2* mutant allele, and complementation of the *pds2* mutant with the *AtHST* cDNA conclusively demonstrate that *pds2* is a mutation in the *AtHST* gene. The subcellular localization of AtHST provides additional evidence supporting chloroplastic synthesis of PQ. The pleiotropic effect

Table 2 Functional complementation of the *Arabidopsis pds2* mutant by *AtHST*

Transgenic lines	Green:white	χ^{2a}	Basta resistant:Basta sensitive	χ^{2b}
pds2/AtHST #1	163:16	2.42 ($P > 0.1$)	115:47	1.62 ($P > 0.2$)
pds2/AtHST #2	280:25	2.01 ($P > 0.1$)	206:58	1.29 ($P > 0.2$)
pds2/AtHST #5	229:21	1.66 ($P > 0.1$)	151:60	1.23 ($P > 0.2$)

Heterozygous *pds2* mutants were transformed with the *AtHST* gene and Basta resistant, *pds2* heterozygous T1 plants were self-pollinated. Segregation analysis was performed with the T2 progenies. The *P* values are indicated in parentheses

[a] Calculated χ^2 values were based on an expected 15:1 ratio

[b] Calculated χ^2 values were based on an expected 3:1 ratio

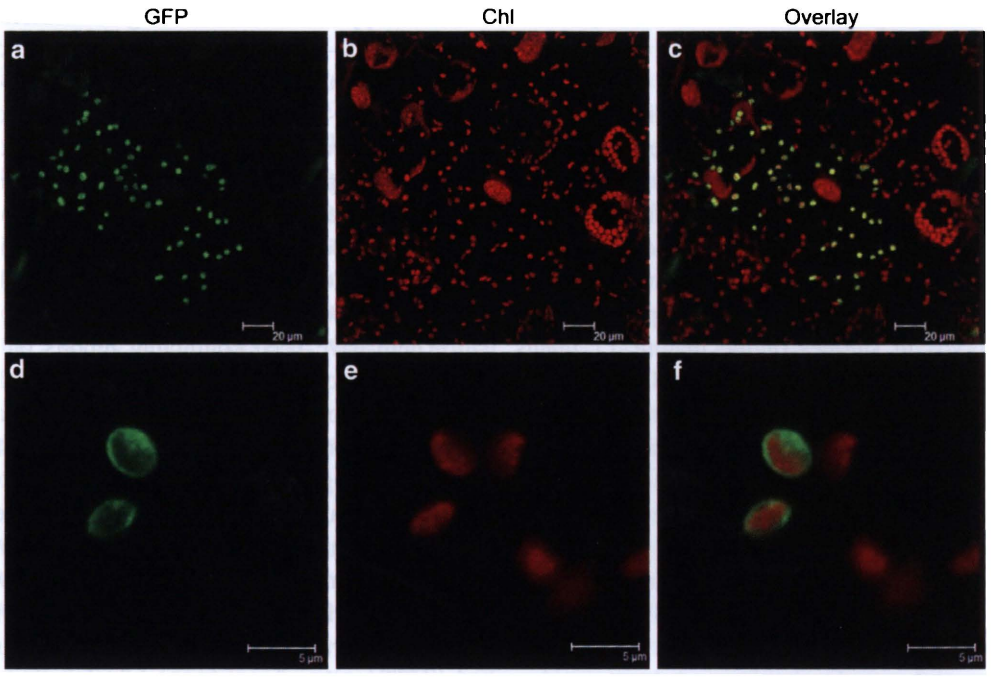

Fig. 3 Confocal micrograph of green fluorescence from EGFP (**a**, **d**), red autofluorescence from chlorophyll (**b**, **e**), and merged green and red signal (**c**, **f**) in an epidermal cell of tobacco expressing the AtHST-EGFP fusion. Figure **d**–**f** are higher magnification images of a single chloroplast from Figs. **a**–**c**, respectively. *GFP* green fluorescence specific for GFP; *Chl* red fluorescence of chlorophylls; *Overlay*, the overlaid image of GFP and Chl

of PQ on tocopherol accumulation, when PQ synthesis/accumulation is perturbed by either the *pds2* mutation or the ectopic expression of *AtHST* (Norris et al 1995; Sadre et al. 2006; Venkatesh et al. 2006), suggests that an interaction exists between the tocopherol and PQ pathways. It remains to be addressed at what level this interaction occurs.

Acknowledgments We thank Dr. Aline Vaster for assistance with confocal microscopy and Drs. Rujin Chen and Ping Xu for critical reading of the manuscript. This work was supported by the Samuel Roberts Noble Foundation.

References

Bräuer L, Brandt W, Wessjohann LA (2004) Modeling the *E. coli* 4-hydroxybenzoic acid oligoprenyltransferase (*UbiA* transferase) and characterization of potential active sites. J Mol Model 10:317–327

Clough SJ, Bent AF (1998) Floral dip: a simplified method for *Agrobacterium*-mediated transformation of *Arabidopsis thaliana*. Plant J 16:735–743

Collakova E, DellaPenna D (2001) Isolation and functional analysis of homogentisate phytyltransferase from *Synechocystis* sp. PCC 6803 and *Arabidopsis* Plant Physiol 127:1113–1124

Emanuelsson O, Nielsen H, Brunak S, von Heijne G (2000) Predicting subcellular localization of proteins based on their N-terminal amino acid sequence. J Mol Biol 300:1005–1016

Garcia I, Rodgers M, Lenne C, Rolland A, Sailland A, Matringe M (1997) Subcellular localization and purification of a *p*-hydroxyphenylpyruvate dioxygenase from cultured carrot cells and characterization of the corresponding cDNA. Biochem J 325:761–769

Hirooka K, Bamba T, Fukusaki E, Kobayashi A (2003) Cloning and kinetic characterization of *Arabidopsis thaliana* solanesyl diphosphate synthase. Biochem J 370:679–686

Hirooka K, Izumi Y, An C, Nakazawa Y, Fukusaki E, Kobayashi A (2005) Functional analysis of two solanesyl diphosphate synthases from *Arabidopsis thaliana*. Biosci Biotechnol Biochem 69:592–601

Liu CJ, Dixon RA (2001) Elicitor-induced association of isoflavone *O*-methyltransferase with endomembranes prevents formation and 7-*O*-methylation of daidzein during isoflavonoid phytoalexin biosynthesis. Plant Cell 13:2643–2658

Murashige T, Skoog F (1962) A revised medium for rapid growth and bioassays with tobacco tissue culture. Physiol Plant 15:473–497

Nicholas KB, Nicholas HB Jr, Deerfield DW II (1997) GeneDoc: analysis and visualization of gene variation. Embnet News 4:1–4

Nielsen H, Engelbrecht J, Brunak S, von Heijne G (1997) Identification of prokaryotic and eukaryotic signal peptides and prediction of their cleavage sites. Protein Eng 10:1–6

Nievelstein V, Vandekerckhove J, Tadros MH, von Lintig J, Nitschke W, Beyer P (1995) Carotene desaturation is linked to a respiratory redox pathway in *Narcissus pseudonarcissus* chromoplast membranes. Involvement of a 23-KDa oxygen-evolving-complex-like protein. Eur J Biochem 233:864–872

Norris SR, Barrette TR, DellaPenna D (1995) Genetic dissection of carotenoid synthesis in *Arabidopsis* defines plastoquinone as an essential component of phytoene desaturation. Plant Cell 7:2139–2149

Norris SR, Shen X, DellaPenna D (1998) Complementation of the *Arabidopsis pds1* mutation with the gene encoding *p*-Hydroxyphenylpyruvate dioxygenase. Plant Physiol 117:1317–1323

Osowska-Rogers S, Swiezewska E, Andersson B, Dallner G (1994) The endoplasmic reticulum–Golgi system is a major site of

plastoquinone synthesis in Spinach leaves. Biochem Biophys Res Comm 205:714–721

Restrepo MA, Freed DD, Carrington JC (1990) Nuclear transport of plant potyviral proteins. Plant Cell 2:987–998

Sadre R, Gruber J, Frentzen M (2006) Characterization of homogentisate prenyltransferases involved in plastoquinone-9 and tocopherol biosynthesis. FEBS Lett 580:5357–5362

Savidge B, Weiss JD, Wong YH, Lassner MW, Mitsky TA, Shewmaker CK, Post-Beittenmiller D, Valentin HE (2002) Isolation and characterization of homogentisate phytyltransferase genes from *Synechocystis* sp. PCC 6803 and *Arabidopsis* Plant Physiol 129:321–332

Siebert M, Bechthold A, Melzer M, May U, Berger U, Schroder G, Schroder J, Severin K, Heide L (1992) Ubiquinone biosynthesis. Cloning of the genes coding for chorismate pyruvate-lyase and 4-hydroxybenzoate octaprenyl transferase from *Escherichia coli* FEBS Lett 307:347–350

Soll J, Kemmerling M, Schultz G (1980) Tocopherol and plastoquinone synthesis in spinach chloroplasts subfractions. Arch Biochem Biophys 204:544–550

Soll J, Schultz G, Joyard J, Douce R, Block MA (1985) Localization and synthesis of prenylquinones in isolated outer and inner membranes from spinach chloroplasts. Arch Biochem Biophys 238:290–299

Swiezewska E (2004) Ubiquinone and plastoquinone metabolism in plants. Methods Enzymol 378:124–131

Swiezewska E, Dallner G, Andersson B, Ernster L (1993) Biosynthesis of ubiquinone and plastoquinone in the endoplasmic reticulum–Golgi membranes of spinach leaves. J Biol Chem 268:1494–1499

Thompson JD, Gibson TJ, Plewniak F, Jeanmougin F, Higgins DG (1997) The Clustal_X windows interface: flexible strategies for multiple sequence alignment aided by quality analysis tools. Nucleic acid Res 25:4876–4882

Tian L, Dixon RA (2006) Engineering isoflavone metabolism with an artificial bifunctional enzyme. Planta 224:496–507

Venkatesh T, Karunanandaa B, Free D, Rottnek J, Baszis S, Valentin HE (2006) Identification and characterization of an *Arabidopsis* homogentisate phytyltransferase paralog. Planta 223:1134–1144

Wanke M, Dallner G, Swiezewska E (2000) Subcellular localization of plastoquinone and ubiquinone synthesis in spinach cells. Biochim Biophys Acta 1463:188–194